

Compressive properties of porous metal fiber sintered sheet produced by solid-state sintering process

Wei Zhou^{a,*}, Yong Tang^b, Bin Liu^b, Rong Song^a, Lelun Jiang^a, K.S. Hui^c, K.N. Hui^d, Haimin Yao^e

^a School of Engineering, Sun Yat-sen University, Guangzhou 510006, China

^b School of Mechanical and Automotive Engineering, South China University of Technology, Guangzhou 510640, China

^c Department of Systems Engineering and Engineering Management, City University of Hong Kong, Hong Kong, China

^d Department of Materials Science and Engineering, Pusan National University, Republic of Korea

^e Department of Mechanical Engineering, The Hong Kong Polytechnic University, Hung Hom, Kowloon, Hong Kong, China

ARTICLE INFO

Article history:

Received 14 July 2011

Accepted 10 September 2011

Available online 17 September 2011

Keywords:

B. Fibers and filaments

C. Sintering

E. Mechanical properties

ABSTRACT

A novel porous metal fiber sintered sheet (PMFSS) with three-dimensional reticulated structure was fabricated by using solid-state sintering method of copper fibers. Uniaxial compressive test was carried out to investigate the effects of porosity and manufacturing parameters on the compressive properties of PMFSS. During the compressive process, it was found that the PMFSS initially exhibited short-term elastic deformation, and then quickly entered into the compact densification deformation stage. The stress–strain plots showed no obvious yield stage in the whole uniaxial compressive process. Under given stress, the PMFSS with higher porosity exhibited higher strain, hence implying lower effective stiffness. Additionally, our results showed that higher sintering temperature or longer sintering time would soften the PMFSS.

Crown Copyright © 2011 Published by Elsevier Ltd. All rights reserved.

1. Introduction

The porous metal fiber sintered sheet (PMFSS), a new type of porous metal materials, has a three-dimensional network structure featuring high porosity and large specific surface area. It has been widely used in the defense and military, petrochemical industry, metallurgical machinery, environmental protection for its excellent performance in filtration and separation [1], fluid distribution [2], energy absorption [3], biomedical device [4], catalytic reaction [5], heat transfer [6], and so on. In recent years, with the extension of its application field and increasing complexity of its working environment, it is important to understand the relationship between structure and properties of PMFSS to widen its application. However, the previous enormous research work focused on the mechanical properties of metal foam including aluminum foam [7], copper foam [8], and other metal foams [9]. There were not many reports available in the literatures that describe the relationship between microscopic structures and mechanical properties of porous fiber material sintered by using stainless steel fibers and wires [10,11].

As for the metal foam, Gibson and Ashby et al. [12,13] successfully developed a theory to predict the elastic modulus and strength as functions of density, as well as the stress–strain relationship under the compressive deformation process. Their theory was verified by a number of experimental results. The follow-up theoretical

study on energy absorption shed much light on the properties of metal foam. Hyun and Nakajima [14] investigated the effect of pore structure on the compressive process of copper foam, and then conducted a preliminary analysis of the energy absorption. Koza et al. [15] started the preliminary research on the compressive process of aluminum foams with different porosities and dimensions. Liu [16,17] developed a theoretical model for the relationship between structural parameters and mechanical characteristics of metal foam with high porosity. A series of experiments were conducted using nickel foams prepared under different conditions, showing good consistence with the theoretical models.

As for the PMFSS, Ducheyne et al. [18] produced a less porous PMFSS using two types of AISI 316L stainless steel fibers with diameters of 50 μm and 100 μm , of which the tensile and compressive properties were studied. Clyne and Markaki [10,19] fabricated highly porous sheets by using liquid phase sintering of short stainless steel fibers with diameter of 100 μm , followed by an electroplating step to coat the surface with a 5 μm thick copper layer. The PMFSS was obtained after sintering the coated copper fibers at temperature of 1100–1200 $^{\circ}\text{C}$ for 5 min, giving rise to high porosity varying from 75% to 95%. And the tensile strength of all sheets was less than 1 MPa. Recently, Qiao et al. [20] fabricated a PMFSS through vacuum sintering of metal fiber with the diameter of 12 μm . The analysis of microscopy morphology was conducted using scanning electron microscopy. Furthermore, the quasi-static compressive properties of PMFSS were studied by using MTS858 system at room temperature [20]. In the present study, the PMFSS

* Corresponding author. Tel./fax: +86 20 39332148.

E-mail addresses: zhouw23@mail.sysu.edu.cn, abczhoulin@163.com (W. Zhou).

with a three-dimensional reticulated structure is produced using the solid-state sintering of copper fibers. The compressive process of PMFSS is investigated by using the uniaxial compressive test. Finally, the effect of the porosity and manufacturing parameters on the compressive properties of PMFSS was studied in detail.

2. Experimental procedure

2.1. Manufacturing process of PMFSS

As reported previously [21], the processing procedure of PMFSS was divided into following five steps: fiber chipping, mold-pressing, sintering, cooling, and testing. First of all, the continuous copper fibers were fabricated by cutting method with a multi-tooth lathe tool. These copper fibers were then cut into segments with the length ranging from 10 to 20 mm. Next, the copper fibers with random directions were uniformly put into the packing chamber of the mold pressing equipment, and then pressure was applied by screwing the bolts. In this way, the semi-finished PMFSS with the same shape as the predetermined packing chamber was obtained. Sintering was carried out in the box-type furnace which provided the hydrogen gas atmosphere with constant pressure of 0.3 MPa. The sintering temperature was in the range from 700 °C to 1000 °C and controlled by a programmable temperature controller. Stage heating method was used to optimize the heating rate. The heating rate was kept at 300 °C/h when the temperature was below 800 °C, while reduced to 200 °C/h as the temperature was above 800 °C. The sintering time was set as either 30 min or 60 min. When the sintering was completed, the sample was removed from the furnace and cooled in air to the room temperature. Finally, the mold pressing equipment was disassembled and the PMFSS was ready for characterization and compressive test.

2.2. Characterization and compressive test of PMFSS

Since the obtained PMFSS has a regular geometric shape, we can calculate the average porosity using the quality–volume method formulated by

$$E(\%) = \left(1 - \frac{M}{\rho V}\right) \times 100, \quad (1)$$

where V is the volume of PMFSS (cm^3) M is the mass of PMFSS (g) and ρ is the density of red copper (g/cm^3).

Scanning electron microscopy (JSM-6380LA, Japan) was adopted to observe the microscopic structure of PMFSS. The compressive test was carried out on an electronics universal testing machine (RGL-20A) with maximum load of 20 kN, performing both test control and data acquisition. To avoid the size effect, the

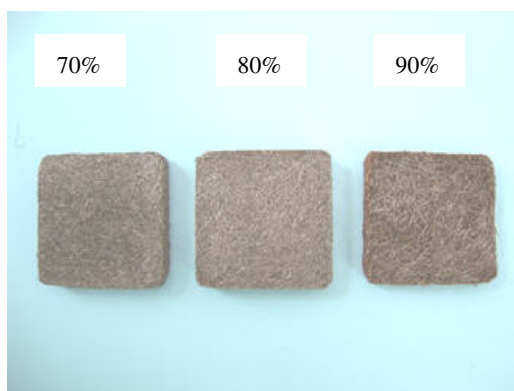


Fig. 1. Photographs of the PMFSS samples with different porosities prepared for compressive test.

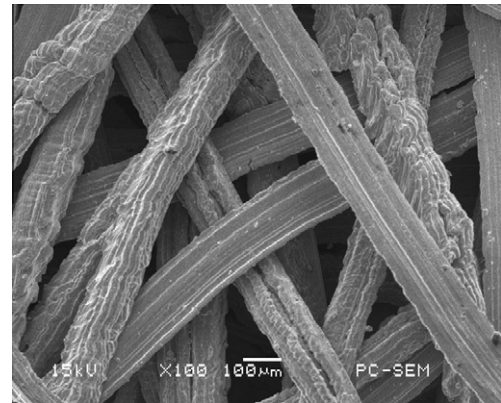


Fig. 2. SEM image of the PMFSS with 80% porosity sintered at 800 °C for 30 min.

minimal length, width, and height of samples are required to be at least seven times larger than the pore size [22]. The value of the average pore size ranges from 100 μm to 1 mm depended on the manufacturing parameters [21]. Therefore, all the PMFSS samples were designed to be 55 mm in length, 55 mm in width, and 10 mm in height. Fig. 1 shows the photographs of the PMFSS samples with different porosities prepared for compressive test. In this study, the compressive process of all test samples was conducted at a constant compressive rate of 1.5 mm/min using the crosshead, which was automatically controlled by the computer software. The load per unit apparent area was taken as the stress. The strains were calculated from the crosshead displacement and the initial measured length of the sample [23]. All the compressive tests were performed at room temperature (approximately 25 °C).

3. Results and discussions

3.1. Microstructures of PMFSS

Fig. 2 shows the SEM image of the PMFSS with 80% porosity sintered at 800 °C for 30 min. As mentioned previously, the copper fibers were distributed randomly in the pressing mold. The pressurization was conducted to produce the mesh structure with many contact regions between the fibers. In the sintering process, the sintering joints between fibers were formed under the set temperature as a result of material migration, and then fiber's metallurgy unification happened, resulting in the PMFSS with three-dimensional reticulated structure. As shown in our previous work [21,24], we found that there were two kinds of sintering joints present in the PMFSS including fiber-to-fiber surface contact and crossing fiber meshing, as shown in Fig. 3a and b, respectively. It was also noted that the PMFSS had a wide porosity range from 60% to 98%, large pore size, and interconnected pores. Moreover, multiscale surface cracks were found on the fibers. These cracks were created during the fabrication process of the fibers. The number of these cracks in the fibers could be reduced by optimizing the fiber's processing parameters. In general, cracks affect the tensile instead of compressive properties of materials [25]. Therefore, here we will not advance further in this aspect but leave the discussion on the crack effect to the future work. In addition, the mechanical properties of PMFSS with three-dimensional reticulated structure can be tailored for different applications by varying the manufacturing parameters of PMFSS.

3.2. Uniaxial compressive process of PMFSS

Uniaxial compressive tests were conducted by using PMFSS fabricated under different manufacturing parameters. The compressed samples exhibited little change in both length and width

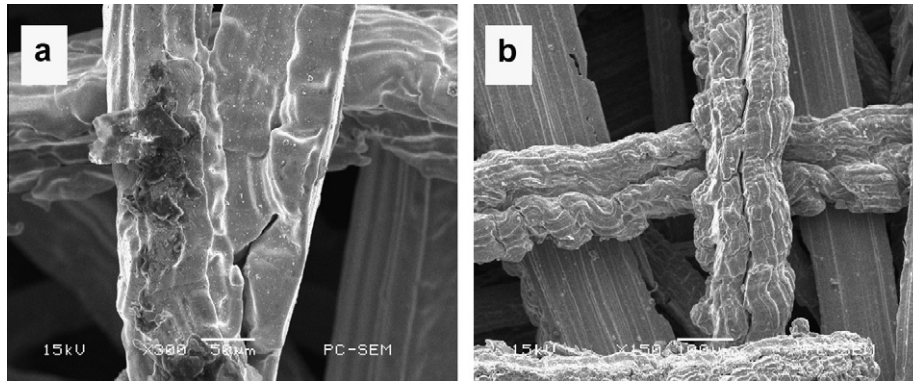


Fig. 3. SEM images of bonding types between fibers in the PMFSS: (a) fiber-to-fiber surface contact and (b) crossing fiber meshing.

Table 1
Dimensions of PMFSS before and after compressive test.

No	Manufacturing parameters	Porosity (%)	Dimension before compression (length × width × height mm)	Dimension after compression (length × width × height mm)
1	Sintering at 800 °C for 30 min	70	55 × 55 × 10	56.1 × 55.5 × 7.56
2	Sintering at 800 °C for 30 min	80	55 × 55 × 10	55.4 × 55.4 × 5.9
3	Sintering at 800 °C for 30 min	90	55 × 55 × 10	54.2 × 55.1 × 3.6
4	Sintering at 800 °C for 60 min	80	55 × 55 × 10	55.6 × 55.1 × 6.12
5	Sintering at 1000 °C for 30 min	80	55 × 55 × 10	55.3 × 55.1 × 6.13

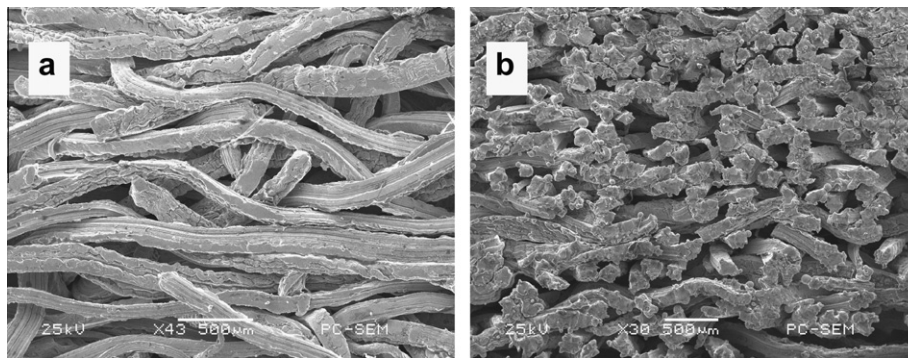


Fig. 4. Microstructures of the PMFSS after uniaxial compressive process (a) top view and (b) cross-section. Sample was sintered at 800 °C for 30 min.

even at large deformation in height compared to the sample without compression. Moreover, it was found that the compressed PMFSS with 70% porosity had the final height of 7.56 mm, and the sample with 90% porosity had the final height of 3.6 mm, as shown in Table 1. Therefore, these experimental results demonstrated that the porosity also has a great impact on the compressive properties. The PMFSS with the lower porosity retains higher height after compressive process. This characteristic of PMFSS provides the convenience for specific application areas with strict requirement of three-dimensional shape. In addition, the height of compressed PMFSS sintered at 800 °C and 1000 °C for 30 min was slightly higher than that sintered at 800 °C for 30 min. Therefore, we conclude that the compressed PMFSS showed small changes in height when the sintering temperature and sintering time are changed. After the uniaxial compressive process, the microstructures of the PMFSS sintered at 800 °C for 30 min are shown in Fig. 4. It can be seen that the three-dimensional reticulated structure of PMFSS disappeared, and a majority of fibers were compressed onto the plane perpendicular to the direction of compressive force, as shown in Fig. 4a. In addition, the SEM image of the cross-section showed that compact densification of PMFSS occurred after compression, as shown in Fig. 4b.

3.3. Effect of porosity on the uniaxial compressive properties

Porosity, as the most intrinsic feature of porous materials, plays an important role in determining the compressive properties of PMFSS [26]. To study the effect of porosity on the uniaxial compressive properties, the PMFSS samples with different porosities fabricated at the same sintering parameters were used to conduct the comparison test. The compressive test samples with three porosities were sintered at 800 °C for 30 min, including 70%, 80%, and 90%. Fig. 5 shows the uniaxial compressive stress–strain plots of the PMFSS sintered at 800 °C for 30 min with different porosities. It is the common trend of the curves that the stress increases gradually with the increasing strain. Under given stress, the PMFSS with higher porosity exhibited higher strain, giving rise to lower effective stiffness. This general trend is consistent with the results of previous study on aluminum foam [15], which implies that porosity is by far the most important variable influencing the mechanical properties of porous metal. Moreover, the PMFSS first experienced a temporary elastic deformation stage, and then directly entered into the compact deformation stage. No yield platform stage was observed throughout the uniaxial compressive process. This behavior is different from that of the metal fiber

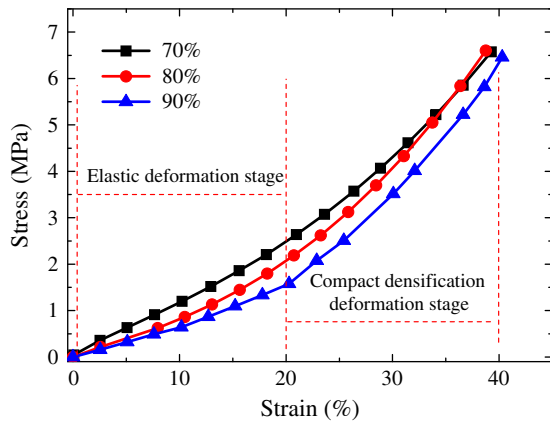


Fig. 5. Uniaxial compressive stress–strain plots of the PMFSS with different porosities. All samples were sintered at 800 °C for 30 min.

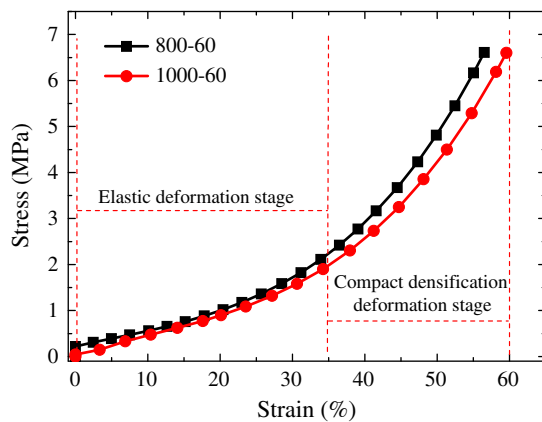


Fig. 6. Uniaxial compressive stress–strain plots of the PMFSS sintered at 800 °C and 1000 °C for 60 min. Both samples have porosity of 80%.

sintered sheet reported in the literature [20]. In general, the compressive process of the porous metal with low density is composed of three stages including linear elastic zone, yield plateau, and densification zone with rapidly increase in the stress [22,27]. The absence of the yield plateau region in our PMFSS may be attributed to the unique three-dimensional reticulated structure of PMFSS with high porosity.

3.4. Effect of manufacturing parameters on the uniaxial compressive properties

Several methods have been developed to produce the porous metal including the melt foaming, sintering, diffusion bonding and welding [10]. However, little has been reported about the relation between the manufacturing parameters and mechanical properties of PMFSS fabricated using the metal fibers [10,11]. Fig. 6 shows the uniaxial compressive stress–strain plots of the PMFSS with 80% porosity sintered at 800 °C and 1000 °C for 60 min. Comparison between Figs. 5 and 6 implies that the elongation of sintering time would soften the PMFSS. Furthermore, the sintering temperature also plays an important role in forming the porous structure during sintering [11]. It can be seen that samples sintered at 800 °C and 1000 °C exhibit similar stress–strain behavior. Under given strain, the stress value for the sample sintered at 800 °C was slightly higher than that for the sample sintered at 1000 °C. Therefore, increasing the sintering temperature could also soften the PMFSS. Such softening mechanism may be attributed to the

combined action of the growth of the sintering joints and the coarsening of grains in the metal fibers [24]. The compressive properties of PMFSS can be tailored according to the applications by varying the sintering temperature and time.

4. Conclusions

The uniaxial compressive test was conducted to study the compressive properties of PMFSS produced by the solid-state sintering process under different manufacturing parameters. In the uniaxial compressive process, the PMFSS initially exhibited short-term elastic deformation, and then directly entered into the compact densification deformation stage. It was found that the PMFSS maintained the three dimensional rectangular shapes after the compressive process. Compared to the sample before compressive procedure, the compressed samples presented the little change both in length and width, but showed the obvious decrease in height. Moreover, the porosity and manufacturing parameters were changed to study the compressive properties of the PMFSS. Our experimental results indicated that the porosity has an important effect on the compressive properties. Under given compressive stress, the PMFSS with higher porosity exhibited larger strain, and therefore lower stiffness. In addition, it was found that increasing the sintering temperature or time would soften the PMFSS. The results obtained in this work will not only help the further development of porous materials, but also provide an important technical guideline for the application of PMFSS in catalysis and acoustic emission.

Acknowledgments

The research work was supported by the National Nature Science Foundation of China (No. 51105387 and 50930005), Natural Science Foundation of Guangdong Province (No. S2011040002152), the Fundamental Research Funds for the Central Universities (No. 11lgpy06) through Sun Yat-sen University, and China Postdoctoral Science Foundation (No. 20100480804). The support from the Foundation of Key Laboratory of Surface Functional Structure Manufacturing of Guangdong Higher Education Institutes in the South China University of Technology (No. SFS-KF201009) is also acknowledged.

References

- [1] Banhart J. Manufacture, characterization and application of cellular metals and metal foams. *Prog Mater Sci* 2001;46:559–632.
- [2] Tang Y, Xiang JH, Wan ZP, Zhou W, Wu L. A novel miniaturized loop heat pipe. *Appl Therm Eng* 2010;30:1152–8.
- [3] Zhang B, Chen TN. Calculation of sound absorption characteristics of porous sintered fiber metal. *Appl Acoust* 2009;70:337–46.
- [4] Lefebvre LP, Banhart J, Dunand DC. Porous metals and metallic foams: current status and recent developments. *Adv Eng Mater* 2008;10:775–87.
- [5] Yuranov I, Kiwi-Minsker L, Renken A. Structured combustion catalysts based on sintered metal fiber filters. *Appl Catal B-Environ* 2003;43:217–27.
- [6] Abduljalil AS, Yu ZB, Jaworski AJ. Selection and experimental evaluation of low-cost porous materials for regenerator applications in thermoacoustic engines. *Mater Des* 2011;32:217–28.
- [7] Brothers AH, Dunand DC. Mechanical properties of a density-graded replicated aluminum foam. *Mater Sci Eng A* 2008;489:439–43.
- [8] El-Hadek AM, Kaytbay S. Mechanical and physical characterization of copper foam. *Int J Mech Mater Des* 2008;4:63–9.
- [9] Liu PS. Mechanical relation for porous metal foams under complex loads of triaxial tension and compression. *Mater Des* 2010;31:2264–9.
- [10] Markaki AE, Gergely V, Cockburn A, Clyne TW. Production of a highly porous material by liquid phase sintering of short ferritic stainless steel fibers and a preliminary study of its mechanical behavior. *Compos Sci Technol* 2003;63:2345–51.
- [11] Liu P, He G, Wu LH. Fabrication of sintered steel wire mesh and its compressive properties. *Mater Sci Eng A* 2008;489:21–8.
- [12] Gibson LJ, Ashby MF, Zhang J, Triantafillou TC. Failure surfaces for cellular materials under multiaxial loads—I. Modeling. *Int J Mech Sci* 1989;31:635–63.
- [13] Andrews E, Sanders W, Gibson LJ. Compressive and tensile behavior of aluminum foams. *Mater Sci Eng A* 1999;270:113–24.

- [14] Hyun SK, Nakajima H. Anisotropic compressive properties of porous copper produced by unidirectional solidification. *Mater Sci Eng A* 2003;340:258–64.
- [15] Koza E, Leonowicz M, Wojciechowski S, Simancik F. Compressive strength of aluminum foams. *Mater Lett* 2003;58:132–5.
- [16] Liu PS, Chen GF. Mechanical relation of foamed metals under uniaxial and biaxial loads of collective tension and compression. *Mater Sci Eng A* 2009;507:190–3.
- [17] Liu PS. Mechanical behaviors of porous metals under biaxial tensile loads. *Mater Sci Eng A* 2006;422:176–83.
- [18] Ducheyne P, Aernoudt E, Meester PD. The mechanical behavior of porous austenitic stainless steel fiber structures. *J Mater Sci* 1978;13:2650–8.
- [19] Tan JC, Clyne TW. Ferrous fiber network materials for jetNoise reduction in aeroengines. Part II: Thermo-mechanical stability. *Adv Eng Mater* 2008;10:201–9.
- [20] Qiao JC, Xi ZP, Tang HP, Wang JY, Zhu JL. Compressive behavior of porous metal fibers. *Rare Metal Mat Eng* 2008;37:2173–6.
- [21] Tang Y, Zhou W, Xiang JH, Liu WY, Pan MQ. An innovative fabrication process of porous metal fiber sintered felts with three-dimensional reticulated structure. *Mater Manuf Process* 2010;25:565–71.
- [22] Ashby MF, Evans T, Fleck NA, Gibson LJ, Hutchinson JW, Wadley HNG. *Metal foams: a design guide*. Woburn (MA): Butterworth-Heinemann; 2000.
- [23] Peroni L, Avalle M, Peroni M. The mechanical behavior of aluminum foam structures in different loading conditions. *Int J Impact Eng* 2008;35:644–58.
- [24] Zhou W, Tang Y, Pan MQ, Wei XL, Xiang JH. Experimental investigation on uniaxial tensile properties of high-porosity metal fiber sintered sheet. *Mater Sci Eng A* 2009;525:133–7.
- [25] Anderson TL. *Fracture mechanics: fundamentals and applications*. 3rd ed. Boca Raton (FL): CRC Press; 2005.
- [26] Liu PS, Li TF, Fu C. Relationship between electrical resistivity and porosity for porous metals. *Mater Sci Eng A* 1999;268:208–15.
- [27] Gibson LJ. Mechanical behavior of metallic foams. *Annu Rev Mater Sci* 2000;30:191–227.